

Design of masonry walls and reinforced concrete columns with column-deflection-curves

Autor(en): **Thürlimann, Bruno / Schwartz, Joseph**

Objektyp: **Article**

Zeitschrift: **IABSE proceedings = Mémoires AIPC = IVBH Abhandlungen**

Band (Jahr): **11 (1987)**

Heft P-108: **Design of masonry walls and reinforced concrete columns with column-deflection-curves**

PDF erstellt am: **27.06.2024**

Persistenter Link: <https://doi.org/10.5169/seals-40368>

Nutzungsbedingungen

Die ETH-Bibliothek ist Anbieterin der digitalisierten Zeitschriften. Sie besitzt keine Urheberrechte an den Inhalten der Zeitschriften. Die Rechte liegen in der Regel bei den Herausgebern.

Die auf der Plattform e-periodica veröffentlichten Dokumente stehen für nicht-kommerzielle Zwecke in Lehre und Forschung sowie für die private Nutzung frei zur Verfügung. Einzelne Dateien oder Ausdrucke aus diesem Angebot können zusammen mit diesen Nutzungsbedingungen und den korrekten Herkunftsbezeichnungen weitergegeben werden.

Das Veröffentlichen von Bildern in Print- und Online-Publikationen ist nur mit vorheriger Genehmigung der Rechteinhaber erlaubt. Die systematische Speicherung von Teilen des elektronischen Angebots auf anderen Servern bedarf ebenfalls des schriftlichen Einverständnisses der Rechteinhaber.

Haftungsausschluss

Alle Angaben erfolgen ohne Gewähr für Vollständigkeit oder Richtigkeit. Es wird keine Haftung übernommen für Schäden durch die Verwendung von Informationen aus diesem Online-Angebot oder durch das Fehlen von Informationen. Dies gilt auch für Inhalte Dritter, die über dieses Angebot zugänglich sind.

Design of Masonry Walls and Reinforced Concrete Columns with Column-Deflection-Curves

Dimensionnement de murs en maçonnerie et de colonnes en béton armé
basé sur l'équilibre de la déformée

Bemessung von Mauerwerkswänden und Stahlbetonstützen
mit Gleichgewichts-Biegelinien

Bruno THÜRLIMANN

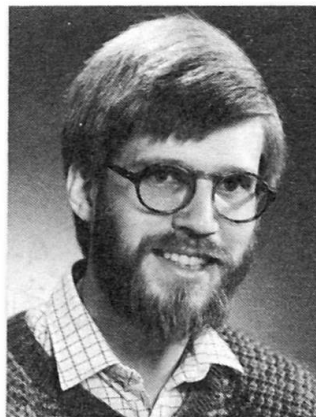
Prof. Dr.
Swiss Fed. Inst. of Technology
Zürich, Switzerland



Bruno Thürlimann obtained a diploma in Civil Engineering from the Swiss Fed. Inst. of Technology in 1946 and a Ph.D. degree from Lehigh Univ., Bethlehem, PA, USA, in 1951. He did research work on the application of the theory of plasticity to the design of steel structures at Lehigh University. Since his return to Switzerland he extended his research to reinforced concrete, prestressed concrete and masonry structures. From 1977 to 1985 he was president of IABSE.

Joseph SCHWARTZ

Research Associate
Swiss Fed. Inst. of Technology
Zürich, Switzerland



Joseph Schwartz studied at the Swiss Federal Institute of Technology. After graduating with a diploma in Civil Engineering in 1981 he is doing research work on masonry structures.

SUMMARY

Numerical and analytical procedures for the determination of column-deflection-curves in the case of a nonlinear moment-curvature relationship are presented. Making use of an affinity relation a simplified procedure for the design of masonry walls and reinforced concrete columns is developed.

RÉSUMÉ

L'article propose des procédures numériques et analytiques pour déterminer la déformée de colonnes soumises à des efforts normaux en considérant un comportement moment-courbure nonlinéaire. En utilisant une relation d'affinité, un concept de dimensionnement simplifié est proposé pour des murs en maçonnerie et des colonnes en béton armé.

ZUSAMMENFASSUNG

Numerische und analytische Verfahren zur Bestimmung von Gleichgewichts-Biegelinien von gedrückten Stäben mit nichtlinearem Momenten-Krümmungsverhalten werden dargestellt. Durch Ausnützung einer Affinitätsbeziehung wird ein vereinfachtes Verfahren zur Bemessung von Mauerwerkswänden vorgeschlagen.



1. COLUMN-DEFLECTION-CURVES WITH A NONLINEAR MOMENT-CURVATURE RELATIONSHIP

1.1 Numerical Integration of the Column-Deflection-Curve (CDC)

Deflection curves of columns with a nonlinear moment-curvature relationship were first developed by W. Ritter 1888 [1]. He solved the problem by graphical methods (Figs. 1,2). T. von Karman 1910 [2] and E. Chwalla 1934 [3] used a numerical procedure and generalized the method for arbitrary boundary conditions.

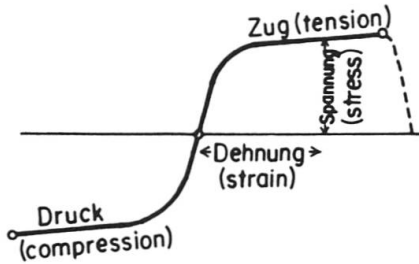


Fig.1 Nonlinear Stress-Strain Relationship (ref.[1])

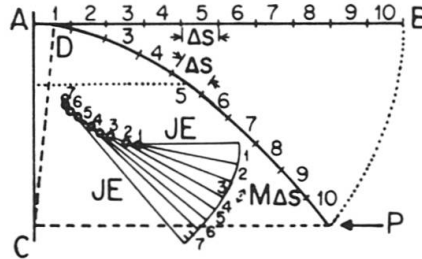


Fig.2 Graphical Construction of the CDC (ref.[1])

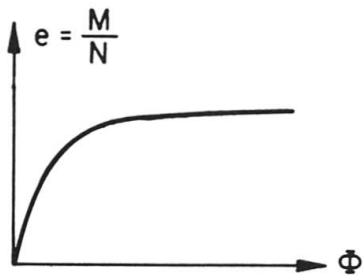


Fig.3 Nonlinear Moment-Curvature Relationship

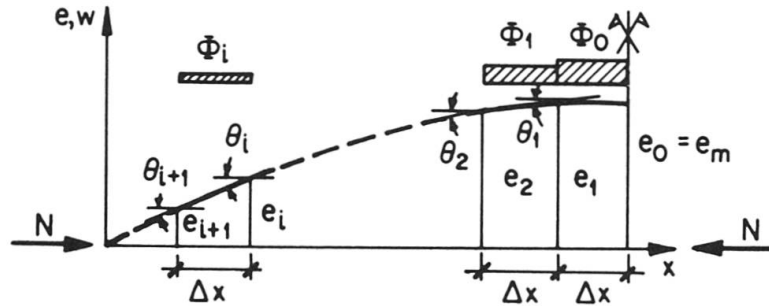


Fig.4 Numerical Construction of the CDC

The moment-curvature relationship $M-\phi$ of a cross section under constant normal force N can be represented as an eccentricity-curvature curve with $M/N=e$, where e corresponds to the eccentricity of the normal force (Fig.3). The curvature ϕ is related to the deflection w of the column by

$$\phi = - \frac{d^2w(x)}{dx^2} \tag{1}$$

and using

$$w(x) = e(x) \tag{2}$$

the column deflection curve (CDC) can be determined by numerical integration (Fig.4) from the equations

$$e_i = e_{i-1} - \phi_{i-1} \cdot \frac{\Delta x^2}{2} - \theta_{i-1} \cdot \Delta x \tag{3}$$

$$\theta_i = \theta_{i-1} + \phi_{i-1} \cdot \Delta x \tag{4}$$

starting with a specific value, for example the maximum eccentricity e_m at mid-span of the column.

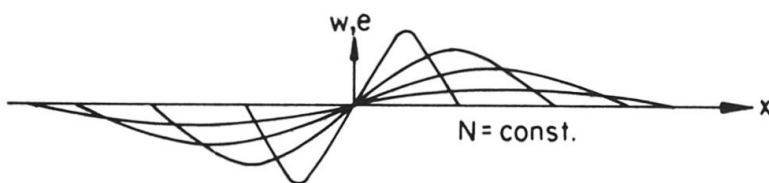


Fig.5 CDC Family

Changing the value of e_m a family of CDC for a constant normal force N can be constructed as shown in Fig.5. Such families of CDC can be directly used for the design of columns.

1.2 Analytical Solutions

Equation (1) relates the curvature of the cross section to the deflection of the column. Using Eq.(2) and introducing a reference eccentricity e_0 , Eq.(1) can be rewritten:

$$-\frac{d^2\eta(x)}{dx^2} \cdot e_0 = \Phi(\eta) \tag{5}$$

with

$$\eta(x) = \frac{e(x)}{e_0} \tag{6}$$

Eq.(5) holds for arbitrary eccentricity-curvature relationships $\Phi(\eta)$ and represents the nonlinear differential equation of the deflection $w(x)=\eta(x) \cdot e_0$ of the beam-column. A direct solution of the equation (5) is generally not possible. Hence the CDC families cannot be represented by elementary analytical functions.

For certain types of eccentricity-curvature relationships however closed form solutions have been recently developed [8]. Assuming that the nondimensional eccentricity η and the curvature Φ are related by the equation

$$\Phi(\eta) = \frac{2 \cdot N \cdot e_0}{(EI)_0 \cdot \pi} \cdot \tan\left(\frac{\pi}{2} \cdot \eta\right) \cdot \left[1 + \tan^2\left(\frac{\pi}{2} \cdot \eta\right)\right] \tag{7}$$

where $(EI)_0$ is the initial flexural stiffness of the cross section with $(N, \Phi=0)$, the solution of the differential equation (5) is:

$$\eta(x) = \frac{2}{\pi} \cdot \sin^{-1} \left[\sin\left(\eta_m \cdot \frac{\pi}{2}\right) \cdot \sin\frac{\pi \cdot x}{l} \right] \tag{8}$$

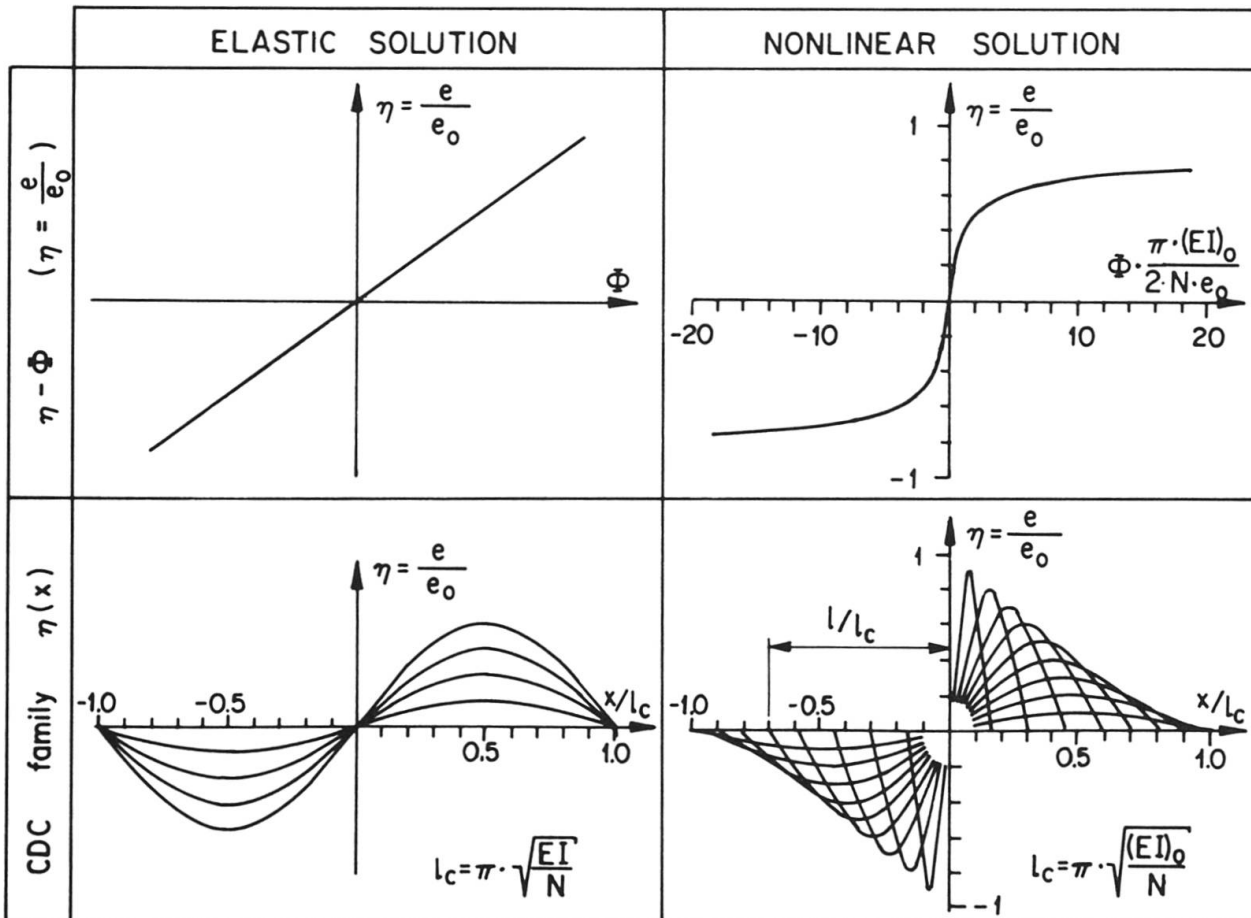


Fig.6 Analytical Solutions



with

$$l = \pi \cdot \left[\frac{(EI)_0}{N} \right]^{1/2} \cdot \cos\left(\eta_m \cdot \frac{\pi}{2}\right). \tag{9}$$

Eq.(5) is satisfied by differentiating Eq.(8) twice with respect to x and substituting x with the inverse function $x(\eta)$ of Eq.(8).

The family parameter η_m is the nondimensionalized eccentricity at $x=1/2$ and l the half-wave-length of the CDC. Equation (9) shows that due to the overproportional increase of the curvature ϕ with the eccentricity η , the length l decreases from the initial critical length $l_c = \pi \cdot [(EI)_0/N]^{1/2}$ for $\eta_m=0$ as a \cos -function $\cos(\eta_m \cdot \pi/2)$. The η - ϕ relationship and the CDC family are shown in Fig.6 for the elastic as well as for the described nonlinear solution.

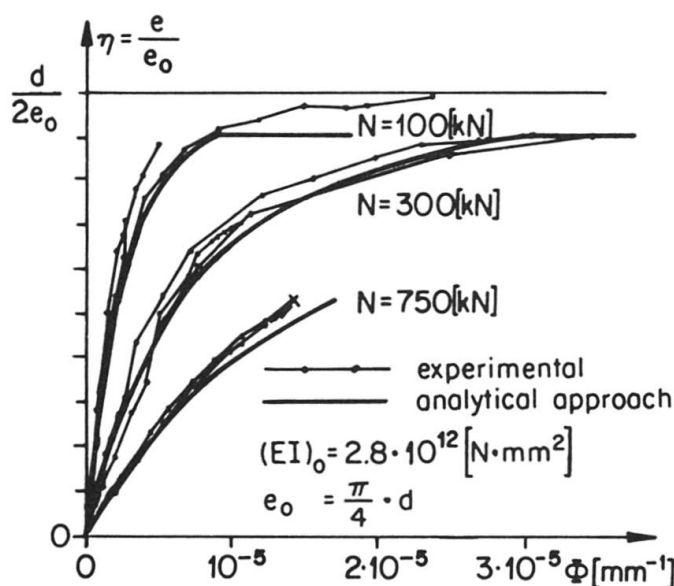
When η_m tends towards zero, the second derivative of the function $\phi(\eta)$ with respect to η becomes zero, i.e. the η - ϕ -relationship becomes linear and the CDC tends towards a sine-wave with a half-wave-length corresponding to the elastic buckling length l_c . The solution is reduced to the classical elastic solution. If the eccentricity e_m tends towards e_0 , i.e. $\eta_m = 1$, the half-wave of the CDC tends towards two linear segments with a concentrated bend at mid-span. For high values of η_m the solution is no longer exact due to the linearization applied to Eq.(1). Such values, however, do not occur in the design of structural columns.

A further analytical solution and combinations with the elastic solution are given in [8].

2. DESIGN OF MASONRY WALLS

2.1 The Eccentricity-Curvature Relationship of Eccentrically Loaded Masonry Walls

The geometrical pattern of the bricks as well as the joints cause an anisotropic behavior of masonry. The joint material, the form of the joints, the cracks strongly influence the behavior and the ultimate strength of masonry walls.



These circumstances make it practically impossible to derive the eccentricity-curvature relationship starting from the stress-strain relationships of the constituent materials (bricks and joints), the pattern of the bricks and the form of the joints. Usually the stress-strain relationship of a fictitious "smeared" material is appropriately calibrated to match the ensuing eccentricity-curvature relationship with experimentally observed e - ϕ curves. It seems more appropriate to calibrate the eccentricity-curvature relationship directly from experimental observations respecting the constraining mechanical relations.

Fig.7 Calibration of η - ϕ Curves

In this way the parameters $(EI)_0$ and e_0 of the presented analytical solution are calibrated by approximating the experimental $e-\phi$ relationship. Fig.7 compares experimental $\eta-\phi$ curves [5] with calibrated analytical curves. In the case of unreinforced masonry the maximum value of the eccentricity cannot exceed $d/2$. The theoretical curves have been limited by a horizontal line at a value of 90 percent of $d/2$ corresponding to $\eta=0.9 \cdot d/2 \cdot e_0$. More refined approaches are discussed in [8].

By assuming a constant value of e_0 for all $\eta-\phi$ curves irrespective of the level of the normal force N this curves are affine with respect to the η axis. This assumption is fairly well confirmed by tests.

2.2 Calculation of the Column Deflection Curves

The experiments described in [5] were performed on 2.5 m high and 0.9 m wide clay brick walls subjected to a constant normal force and a progressive rotation of the bottom end up to failure (Fig.8a).

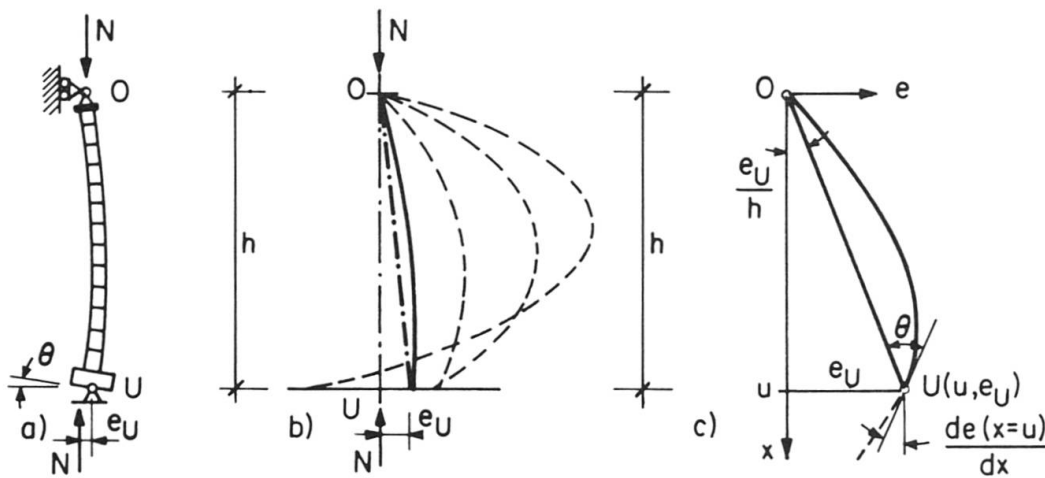


Fig.8 Calculation of $\eta-\theta$ Curves

In Fig.8b the fitting of a wall of height h into a particular CDC is shown with the boundary condition $e=0$ at the top. Using the analytical expression for this particular curve the values e_u and θ as shown in Fig.8c can be determined. At the bottom end the eccentricity of the normal force is:

$$e_U = e(x=u) \tag{10}$$

and the angle of rotation of the wall is expressed by:

$$\theta = \frac{e_U}{h} - \frac{de(x=u)}{dx} \tag{11}$$

By varying the η_m value of a CDC family ($N=\text{constant}$) the $e_u-\theta$ relationship is determined. In Fig.9 theoretical $e_u-\theta$ curves for different levels of N are compared with corresponding experimental curves taken from reference [5].

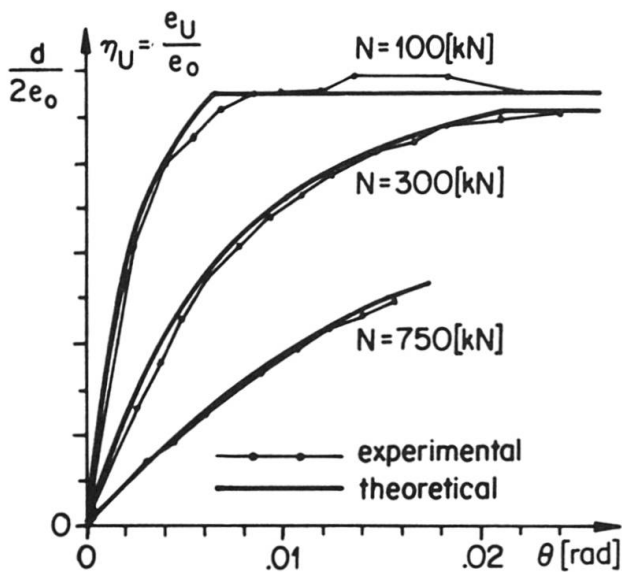


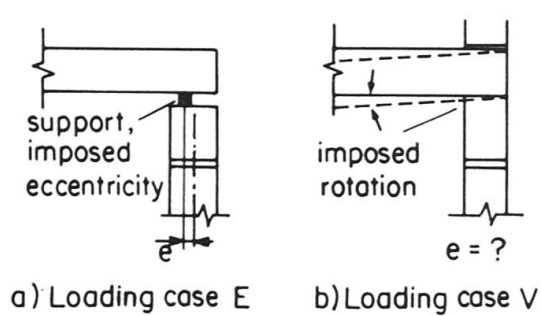
Fig.9 Comparison of $\eta_U-\theta$ Curves



2.3 Design of Masonry Walls Subjected to Normal Forces

2.3.1 Introduction

Two basic loading cases shown in Fig.10 are distinguished. In the case a) the eccentricity at the end of the wall is prescribed and the wall can be designed as an eccentrically loaded column. In case b) the imposed rotation of the slab produces an end moment. Usually the corresponding eccentricity is estimated in order to reduce case b) to case a).



A more appropriate design procedure is presented in [7] which is directly based on the imposed end rotations for three special boundary conditions of the wall. The procedure makes use of a set of auxiliary graphs. Here a simplification of the design method is suggested using the assumption that the eccentricity-curvature curves corresponding to different normal forces are affine as discussed in chapter 2.1.

Fig.10 Loading Cases

2.3.2 Determination of the Eccentricity of the Normal Force

The mentioned auxiliary graphs are given in [7] for three extreme cases of imposed end rotations, V1 to V3 represented in Fig.11. They allow the calculation of four specific values of the bending moment M_W in function of the angle of rotation at the end of the wall (Fig.12). The resulting $M_W-\theta$ curve corresponding to the case V2 is identical to the appropriate $\eta_U-\theta$ curve shown in Fig.9. The $M_D-\theta$ curve represents the bending moment of the slab in function of the end rotation. The common point of the two curves $M_W(\theta)$ and $M_D(\theta)$ conforms to the resultant angle of rotation θ_v of the joint and the bending moment M_v at the end of the wall.

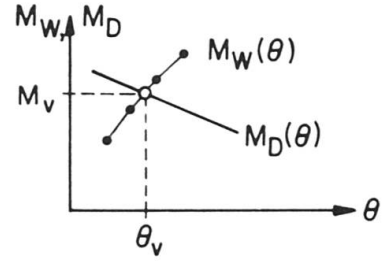
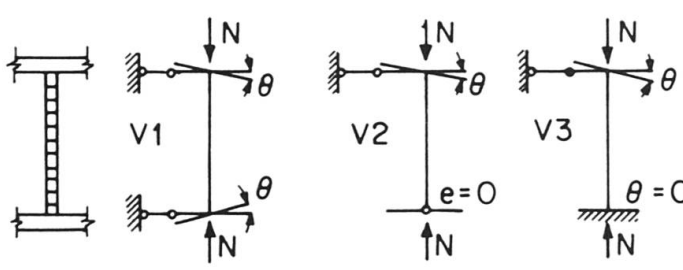


Fig.11 Extreme Cases of Imposed Rotations

Fig.12 Wall-Slab Interaction

Assuming that all the $\eta-\phi$ curves for different values of the normal force, the initial stiffness and the wall-thickness are affine with respect to the η -axis (compare Eq.(7) and Fig.7), a single set of $M_{W_0}(\theta_0)$ curves can be determined using appropriately transformed values of the normal force, the bending moment and the angle of rotation (N_0, M_{W_0}, θ_0) . Such a set is shown in Fig.13a which can be directly used for the design of masonry walls.

2.3.3 The Theoretical Crack Width

The analytical expression of the CDC allows the determination of the maximum curvature and the corresponding maximum crack width r concentrated in a bed joint. Fig.13b) shows $r_0-\theta_0$ curves using the transformed values of the normal force, the crack width and the end rotation angle (N_0, r_0, θ_0) . The resulting crack width r is proportional to the distance c of the bed joints.

2.3.4 Design Concept

The ultimate limit state and the serviceability limit state have to be considered. The first is characterized by instability of the wall or by local collapse of the material under factored loads. Serviceability is checked by an estimate of the theoretical crack width under service loads.

Stability failure is excluded when a common point of the $M_{W_0}-\theta_0$ curve of the wall and the $M_{D_0}-\theta_0$ curve of the slab for the loading cases V (enforced end rotation of the wall) exists or when $M_{W_0}=N_0 \cdot e$ is situated on the $M_{W_0}-\theta_0$ curve for the loading cases E (defined eccentricity of the normal force at the end of the wall). The cross sectional strength imposes limits on the end rotation θ . The maximum theoretical crack width in a bed joint is given in the $r_0-\theta_0$ graph.

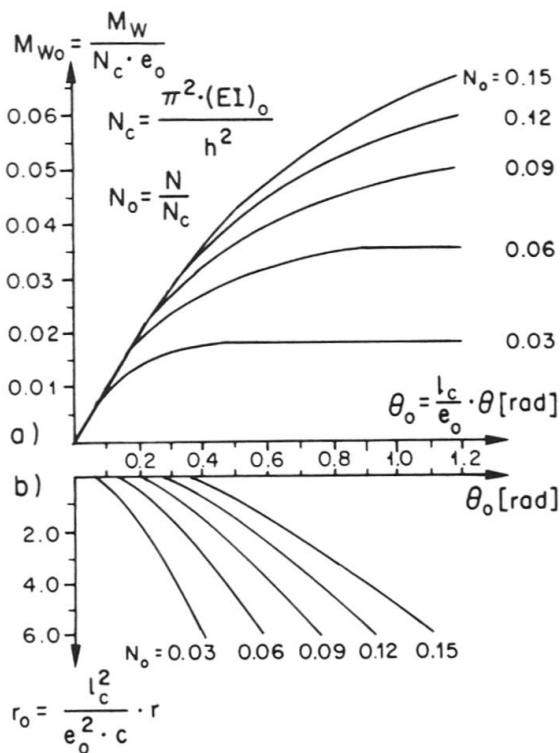


Fig.13 Design Graph

3. DESIGN OF REINFORCED CONCRETE COLUMNS

3.1 Moment-Curvature Relationship

Using a second order parabolic-perfectly plastic stress-strain relationship for concrete (Fig.14) and an elastic-perfectly plastic relationship for reinforcing steel, the $M-\phi$ curves can be computed numerically for different levels of the normal force N . Such $M-\phi$ curves have been computed for the rectangular cross section of an experimentally tested beam (specimen SC-11, [10]). Figure 15 shows the ultimate moment-normal force interaction of the same cross section, assuming a rigid-plastic behavior of both materials. The following investigation is limited to normal forces varying between N_1 and N_{max} .

Figure 16 compares the numerically computed $M-\phi$ curves to approximate curves using the analytical solution, Eq.(7). The parameters $(EI)_0$ and e_0 in Fig.16 have been calibrated in order to match the numerical $M-\phi$ curves. $(EI)_{0,max}$ is the flexural stiffness for $\phi=0$ and N_1 defined in Fig.15. The analytical curves are cut off at a value of $0.8 \cdot M_r/M_{max}$. The experimentally determined curve with $N/N_{max}=0.62$ [10] is compared to the corresponding analytical solution.

Equation (8) gives the analytical expression of the column-deflection-curves for the design of columns.

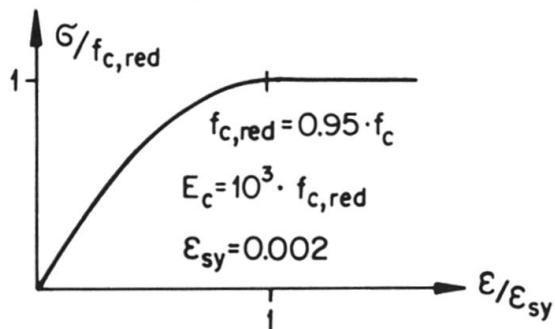


Fig.14 Concrete Stress-Strain Relationship

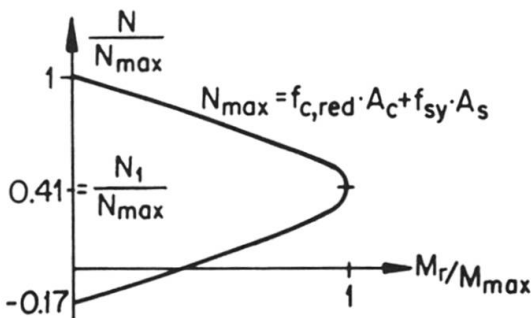


Fig.15 Ultimate Moment-Normal Force Interaction

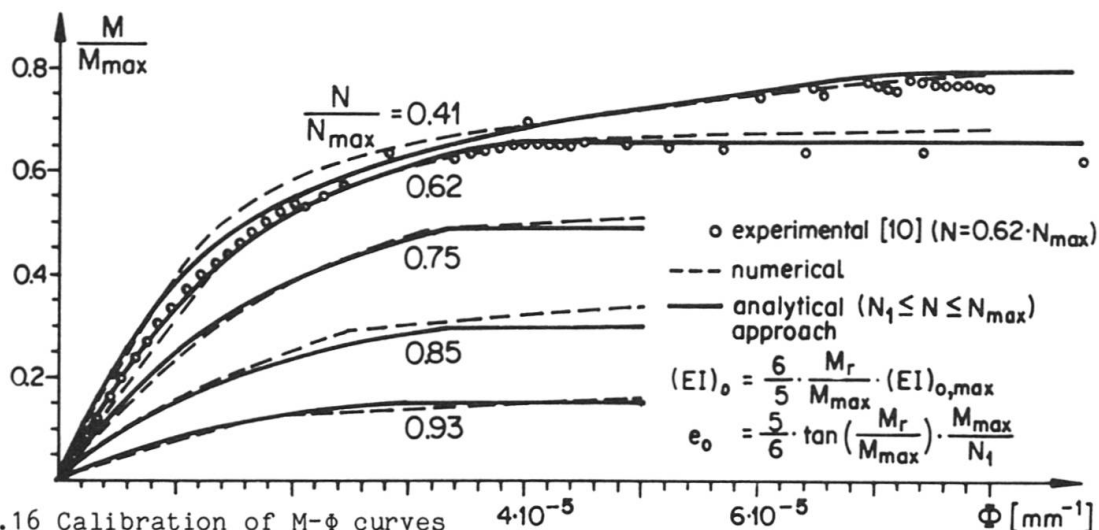


Fig.16 Calibration of M- ϕ curves

3.2 Analytical Design Procedure

The final aim is the development of an analytical column design procedure using simplifications suggested by the affinity of M- ϕ curves. For this a systematic numerical analysis of the main parameters (f_c , N , reinforcement ratio, cross sectional shape) and a comparison with the results of deformation controlled tests are necessary.

DEDICATION

This article is dedicated to Prof. Dr.-Ing. Herbert Kupfer, Technical University of Munich, FRG, on the occasion of his 60th birthday.

REFERENCES

1. RITTER W., Anwendungen der graphischen Statik, Verlag von Meyer & Zeller, Zürich, 1888.
2. VON KARMAN T., Untersuchungen über Knickfestigkeit, Mitteilungen und Forschungsarbeiten V.D.I., 81, Berlin, 1910.
3. CHWALLA E., Theorie des aussermittig gedrückten Stabes aus Baustahl, Der Stahlbau, Oktober 1934.
4. CHEN W.F. and ATSUTA T., Theory of Beam Columns, Volume 1, Mc Graw-Hill, New York, 1976.
5. FURLER R. and THÜRLIMANN B., Versuche über die Rotationsfähigkeit von Backsteinmauerwerk, IBK, ETH Zürich, Bericht Nr. 7502+2, Birkhäuser Verlag Basel und Stuttgart, 1980.
6. FURLER R., Tragverhalten von Mauerwerkswänden unter Druck und Biegung, IBK, ETH Zürich, Bericht Nr. 109, Birkhäuser Verlag Basel und Stuttgart, 1981.
7. Schweizerischer Ingenieur- und Architektenverein (SIA), Empfehlung 1 der Norm SIA 177 "Bemessung von Mauerwerkswänden unter Druck und Biegung", Zürich, 1983.
8. SCHWARTZ J., Zur Bemessung von Mauerwerkswänden und Stahlbetonstützen unter Normalkraft, (to be published).
9. SCHWARTZ J. and THÜRLIMANN B., Versuche über die Rotationsfähigkeit von Zementsteinmauerwerk, IBK, ETH Zürich, Bericht Nr. 8401-1, Birkhäuser Verlag Basel und Stuttgart, 1986.
10. FORD J.S., CHANG D.C. and BREEN J.E., Behavior of Concrete Columns Under Controlled Lateral Deformation, ACI Journal, V. 78, No. 1, 1981.